

# A novel approach describing struvite crystal aggregation and granulation in the fluidized bed for phosphorus recovery from swine wastewater

Zhi-Long Ye, Yujun Deng, Xin Ye, Jie Wu and Shaohua Chen\*

Key Laboratory of Urban Pollutant Conversion, Institute of Urban Environment, Chinese Academy of Sciences, No. 1799 Jimei Road, Xiamen City, Fujian 361021, China.

(E-mail: [zlye@iue.ac.cn](mailto:zlye@iue.ac.cn); [yjdeng@iue.ac.cn](mailto:yjdeng@iue.ac.cn); [xye@iue.ac.cn](mailto:xye@iue.ac.cn); [jwu@iue.ac.cn](mailto:jwu@iue.ac.cn); [shchen@iue.ac.cn](mailto:shchen@iue.ac.cn) )

\*Corresponding author:

Tel: +86 592 6190995; Fax: +86 592 6190977; E-mail address: [shchen@iue.ac.cn](mailto:shchen@iue.ac.cn)

## Abstract

Fluidized bed is commonly used for struvite ( $\text{MgNH}_4\text{PO}_4 \cdot 6\text{H}_2\text{O}$ ) recovery from wastewater. However, effective methods are lacking to describe the properties of the millimeter-scale struvite pellets in the fluidized bed, with the consequence of not predicting and optimizing the granulation process effectively. In this work, swine wastewater was used as the medium for struvite recovery by using fluidized bed reactor. A method combining with image processing and composition analysis was adopted to describe the aggregation and granulation stages of struvite crystal evolution. Based on this method, the properties of struvite granules, including granule type, particle size distribution, number density, mass concentration and crushing strength, were evaluated. Accordingly, the growth rates of the granules, including population growth, mass increase and particle size enlargement, were also determined. It was observed that struvite particles in the fluidized bed evolved into four stages, including aggregation, aggregate compaction, cluster-agglomerating and coating growth. Up-flow rates of 30-80 mm/s in the fluidized bed sustained 600-876 g/L granular solids. Different from the conventional gas-solid granulation models, these stages could occur simultaneously or subsequently. Results revealed that the coating-growth granules were formed with compact aggregates or cluster-agglomerating granules as the nuclei. A novel model for struvite granulation was developed.

## Keywords

Struvite; granulation; wastewater; phosphorus recovery; fluidized bed

## INTRODUCTION

Due to rapid economic growth and urban expansion, a dramatic increase of phosphorus and ammonium discharge from livestock wastewater into the environment has become one of the major issues that many countries have to face. However, from another perspective, such numerous discharge of nitrogen and phosphorus poses great potential for nutrient recovery, especially for struvite ( $\text{MgNH}_4\text{PO}_4 \cdot 6\text{H}_2\text{O}$ ) recovery (Gilbert, 2009; Ye et al., 2011).

Among the technologies of struvite recovery, fluidized bed is preferable because solid and liquid retention times are not systematically similar, and millimeter-scale granules with high purity can be continuously harvested (Le Corre et al., 2009; Forrest et al., 2008; Fattah et al., 2012; Pauli-Bruns et al., 2010). Although fluidized bed have been commercially applied in struvite recovery, such as Ostara Pearl and Phosnix, the design and operation of industrial-scale reactors still requires reliable knowledge originated from lab-scale experiments (Fattah et al., 2012; Rahaman et al., 2014), which may pose problems at the scale-up stage or at process control and optimization (Hemati et al., 2003; Rahaman et al., 2014). Such status indicates that the struvite granulation mechanism is not comprehensively understood.

Previous studies reported that struvite pellets harvested possessed various shapes and structures, such as crystal aggregates, tight agglomerates, granules with inner core and outer shell, and granules consisting of loose crystals (Huang et al., 2006; Forrest et al., 2008; Fattah et al., 2012). Defining the types of struvite granules and determining their corresponding operational conditions are very crucial and practical, so that the operational states of fluidization can be effectively described and the growth rates of solid contents can be well determined. However, limited literature has dedicated on the relevant works. Such current situations indicate that the evolution stages of struvite granules and the granulation mechanisms in fluidized bed are still unclear. Besides, the recovered struvite granules are normally in millimeter-scale size (Forrest et al., 2008; Fattah et al., 2012), which normally require appropriate methodologies to evaluate particle size distribution, either off-line or on-line. Nevertheless, the widely applied off-line method is manual sieving (Forrest et al., 2008; Fattah et al., 2012; da Silva et al., 2014), which is very precise but do not give real information on the particle size distribution inside the fluidized bed. Also, the determination of granule evolution process is still a great challenge for sieving method. Hence, other methods should be implemented to describe the granulation process.

The objective of this study was to develop an original methodology coupling with image processing and composition analysis to describe the aggregation and granulation of struvite crystal evolution in the fluidized bed. The important parameters, including granule type, particle size distribution, granule growth rate, granule number density etc., were determined. Afterwards, an evolution model of struvite granulation was put forward, and the relevant mechanisms were discussed.

## **MATERIALS AND METHODS**

### **Swine wastewater**

Swine wastewater was obtained from an anaerobic digester in an intensive pig farming plant located in Xiamen City, China. The supernatant characteristics during the period of the study were shown in Table S1.

### **Process description and operation**

Referencing to the description of Iqbal et al. (2008) and Fattah et al. (2012), a lab-scale struvite recovery reactor with three sections was designed and constructed. The inside diameters of the crystallizer were 50, 70 and 100 mm, for the bottom, middle and top sections, respectively. The settling section for fine particles was set at the top of the reactor with 400 mm diameter. The volume and height of the crystallizer were approximately 25 L and 180 cm, respectively.

The experimental system was operated over a 4-month period. The influent of wastewater was set at 100 L/d and was fed into the bottom of the reactor. Hydraulic loading was stepwise set at 203.3, 271.1, 338.8, 406.6, 474.4 and 542.1 L/(d·L) by increasing the recycling stream, so as to ensure the up-flow velocity at 30, 40, 50, 60, 70 and 80 mm/s, respectively. MgCl<sub>2</sub> solution was added to supply the desired Mg/P molar ratio in the reactor. During the experiments, pH values were set at 9.0-9.2 by dosing NaOH as the neutralizing agent.

### **Analytical methods**

Wastewater analyses were performed according to the standard methods (APHA, 1998). The collected granules samples were firstly grinded and sifted through mesh sieve, and then the powder was subjected to X-ray diffraction (X'Pert PROMPD, Holland), Fourier transform infrared (FTIR) spectroscopy (Nicolet iS10, ThermoFisher, USA) and Total organic carbon (TOC) analyzer (TOC-V CPH, Shimadzu, Japan). Afterwards, the samples were dissolved by 0.5% HNO<sub>3</sub>, following 0.45 μm membrane filtration. The supernatants were collected for elemental analyses according to the standard methods (APHA, 1998). The solid mass concentrations in different sections of the fluidized bed were determined by using a fixed-volume vessel. The crushing strength of granules

was analysed by a strength tester machine (Autograph AGS-X, Shimadzu, Japan).

### Morphology and particle size distribution

Considering that sieving is not suitable to describe particle size distribution and laser diffraction is proper to nano- and micron-scale particles, image processing was implemented in this study. A digital SMZ-168 TL stereomicroscope (MOTIC China Group Co., Ltd.), equipped with image processing software of Nikon NIS-Elements BR 2.30 (Nikon Instruments Co. Ltd., Japan), was used to assay the morphology of aggregates and granules withdrawn from different sections of the fluidized bed, including area, equivalent diameter, perimeter, macro axis and minor axis. The size distribution of aggregates and granules was determined through statistical analysis on the equivalent diameter of aggregates using Excel 2007 (Microsoft Co. Ltd., USA) software. Scanning electron microscopy (SEM, HITACHI S-4800, Japan) equipped with energy-dispersive spectrometry (EDS, HORIBA 7593-H, Japan) was also adopted to obtain the morphology of the aggregates and granules.

## RESULTS

### Reactor performance

The concentrations of phosphate ( $\text{PO}_4\text{-P}$ ), total phosphorus (TP), ammonia nitrogen ( $\text{NH}_4\text{-N}$ ) and total nitrogen (TN) in the influent and effluent were determined. Phosphate and TP removal kept stably above 94% and 75%, respectively. Detailed results were shown in Figures S1 and S2 (see Supplementary File).

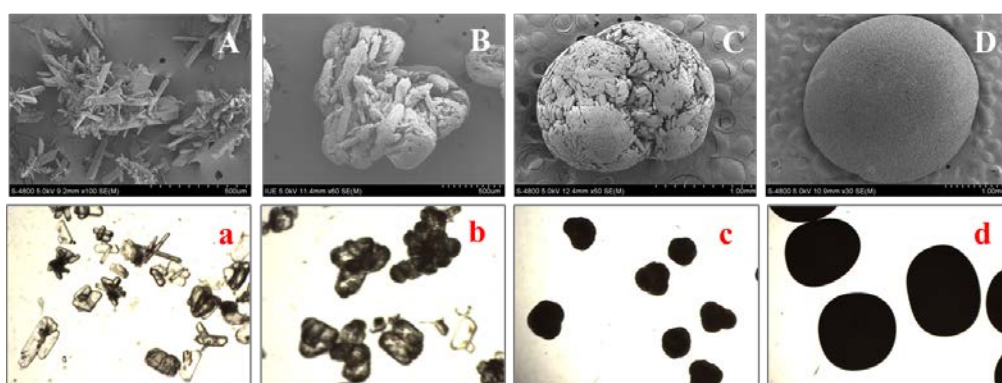


**Figure 1.** Various shapes of struvite particles in the reactor. SEM images: A, aggregates; B, compact aggregates; C, cluster-agglomerating granule; D, coating-growth granule. Images of stereo microscope: a, aggregates, 20-times enlargement; b, compact aggregates, 20-times enlargement; c, cluster-agglomerating granule, 10-times enlargement; d, coating-growth granule, 7.5-times enlargement.

### Physical properties of aggregates and granules

#### Morphology

Figure 1 provided typical images of struvite particles observed in different sections of the fluidized bed. Loose and compact aggregates (Figure 1 A and a, Figure 1 B and b), formed with needle-shaped or rod-shaped crystals, were found in the top and middle sections on the conditions of up-flow rate less than 30 mm/s (Table 1). When up-flow rate increased from 30 mm/s to 80 mm/s, granules containing several clusters emerged in the middle and bottom sections (Figure 1 C and c). This type of pellets was defined as cluster-agglomerating granules. Once up-flow rates exceeded 40.8 mm/s, smooth granules with the construction of loose interior and tight exterior were observed in the middle and bottom sections (Figure 1 D and d). Considering the exterior of the granules was coating by several layers of fine crystals (Figure S3), this type of granules was defined as coating-growth granules. Figure 2 provided the morphology evolution of the granules in different sections

of the fluidized bed. It was obvious that increasing up-flow rates caused shape shifts from aggregates to compact aggregates in the top section, from compact aggregates to cluster-agglomerating granules in the middle section, and from cluster-agglomerating granules to coating-growth granules in the bottom section. Such changes were also recorded in Table 1.

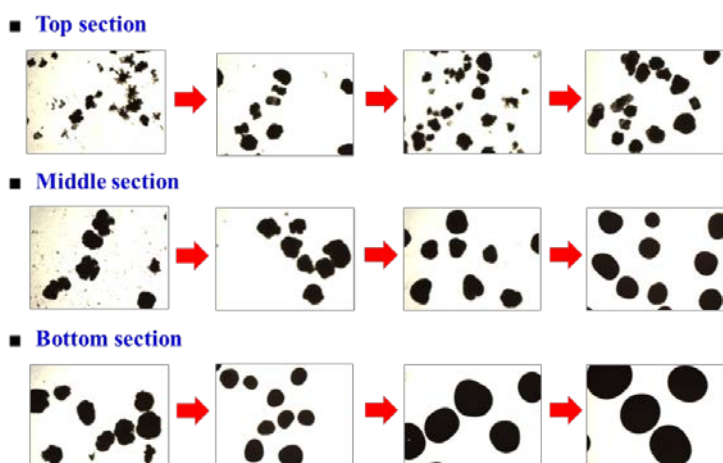


**Figure 2.** Evolution process of struvite particles observed in different sections of the fluidized bed.

#### *Particle size and concentration*

The particle diameter distribution in different sections of the reactor was illustrated in Figure 3. Compared to top and middle sections, higher diameter values and wider size distribution were observed for the pellets at the bottom section. The equivalent diameter ( $d_{0.5}$ ) at the bottom section, combined with up-flow rate, particle shape and solid concentration were summarized in Table 1. Trends were detected in which higher up-flow rates corresponded to higher particle sizes and mass concentrations. It was observed that 30-80 mm/s up-flow rates could sustain 600-876 g/L granular solids in the reactor and harvest pellets with the size range of 1.186-1.872 mm at the bottom section.

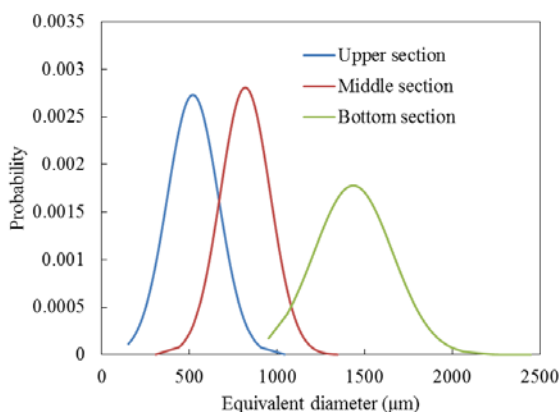


**Figure 3.** Particle size distribution in the fluidized bed at 50 mm/s up-flow rate.

Particle number density was also an important parameter for struvite granulation. Due to the aggregates were too fragile to be collected and measured, cluster-agglomerating and coating-growth granules were harvested for particle number counting. As presented in Table 1, improving up-flow rates resulted in different reduction modes of number density. A gradual reduction pattern was detected on the transformation of cluster-agglomerating granule to coating-growth granule, as presented in the bottom section from Run 2 to Run 6. On the contrary, compact aggregates and cluster-agglomerating granules favoured drastic reduction as shown in the middle section at Run 3, 4, 5 and 6, and the bottom section at Run 1 and 2.

**Table 1.** Experimental details of struvite particles under different up-flow rates.

Run	Unit	1	2	3	4	5	6	
Bottom section	Up-flow rate	(mm/s)	30.0	40.0	50.0	60.0	70.0	80.0
	$d_{0.5}$ <sup>a</sup>	( $\mu\text{m}$ )	1185.7	1496.5	1435.8	1746.6	1656.7	1871.8
	Crushing strength <sup>b</sup>	(N)	1.79	4.33	4.64	7.59	9.54	12.61
	Mass concentration	(g/L)	693.74	600.63	777.13	876.20	863.77	820.13
	Number density	(n/L) <sup>c</sup>	100418	57529	55924	42319	39334	20605
	$v_m$ <sup>f</sup>	g/(L·d)	-	-6.65	12.61	7.08	-0.89	-3.12
	$v_n$ <sup>f</sup>	n/(L·d)	-	3064	115	972	213	1338
	$v_r$ <sup>f</sup>	$\mu\text{m}/(\text{L}\cdot\text{d})$	-	22.2	-4.3	22.2	-6.4	15.4
	Particle shape <sup>d</sup>		CA+CL(<50%)	CL	CL+CT(<25%)	CL+CT(<50%)	CL+CT(~50%)	CL(<50%)+CT
Middle section	Up-flow rate	(mm/s)	15.3	20.4	25.5	30.6	35.7	40.8
	$d_{0.5}$	( $\mu\text{m}$ )	563.9	674.1	820.3	962.9	1051.5	1174.0
	Mass concentration	(g/L)	521.86	577.31	583.12	609.13	656.29	1010.95
	Number density	(n/L)	- <sup>e</sup>	-	308082	189763	163945	95607
	$v_m$	g/(L·d)	-	3.96	0.42	1.86	3.37	25.33
	$v_n$	n/(L·d)	-	-	-	8451	1844	4881
	$v_r$	$\mu\text{m}/(\text{L}\cdot\text{d})$	-	7.9	10.4	10.2	6.3	8.8
		Particle shape		AG	CA	CA+CL(<25%)	CA+CL(<50%)	CL
Top section	Up-flow rate	(mm/s)	7.5	10.0	12.5	15.0	17.5	20.0
	$d_{0.5}$	( $\mu\text{m}$ )	347.9	609.1	520.9	703.5	982.9	1341.6
	Mass concentration	(g/L)	203.54	267.27	329.25	377.90	349.84	372.13
	Number density	(n/L)	-	-	-	-	-	-
	$v_m$	g/(L·d)	-	4.55	4.43	3.48	-2.00	1.59
	$v_n$	n/(L·d)	-	-	-	-	-	-
	$v_r$	$\mu\text{m}/(\text{L}\cdot\text{d})$	-	18.7	-6.3	13.0	20.0	25.6
		Particle shape		AG	AG	AG	CA	CA

<sup>a</sup>  $d_{0.5}$  is the equivalent diameter distribution of the particles.

<sup>b</sup> Considering aggregates in the top section and middle section are very fragile, granules in bottom section are adopted for crushing strength measurement.

<sup>c</sup> The unit of number density, n/L, means that a liter of liquid contains a certain number of granules.

<sup>d</sup> In the column of “Particle shape”, AG is aggregates; CA is compact aggregates; CL is cluster-agglomerating granules; CT is coating-growth granules; “CL(<50%)” means the number of coating-growth granules are less than 50% of the total.

<sup>e</sup> “-” indicates that the aggregates are too fragile to be measured.

<sup>f</sup>  $v_m$ , mass growth rate, determined by the mass increase averaging over the transition time;  $v_n$ , number reduction rate, calculated by the number reduction averaging over the transition time;  $v_r$ , radius growth rate, measured by the radius augment averaging over the transition time.

### Crushing strength

Since the aggregates were very fragile and their strength were hard to be measured, cluster-agglomerating and coating-growth granules generated in the bottom section were harvested for crushing strength determination. As shown in Table 1, enhancing up-flow rates from 30 mm/s to 80 mm/s significantly increased the strength from 1.79 to 12.61 N. It should be noted that different particle shapes displayed significantly different crushing-resistance abilities. The particle strengths augmented more than 6 times, from 1.79 to 12.61 N (Table 1), despite the particles evolution from aggregates to coating-growth with insignificant  $d_{0.5}$  increase (less than 1 mm).

Previous study has reported that the granular particle strictly obeyed the rule that larger granules had higher crushing strength (Walker et al., 1997). Fattah et al. (2012) found that a positive linear relationship existed when the pellets were less than 2.36 mm, whereas a decreasing pattern of strength was observed when the pellet size was beyond 2.36 mm. In the present study, granule structure was found as the key factor for strength augmentation, despite the particle size variation. As illustrated in Figure 4, the cluster-agglomerating granule possessed several small peaks with approximate strength values, indicating that the individual cluster in the granule contributed the major strength of the whole granule. However, the coating-growth granules showed a completely different profile, firstly with a distinct and high peak, and then following with several small peaks. Such crushing profile confirmed that the outer shell of the granule contributed the major strength to resistant breakage.

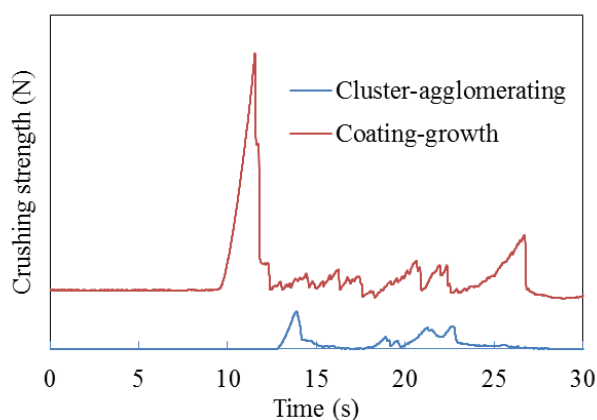


**Figure 4.** Crushing strengths of cluster-agglomerating and coating-growth struvite granules.

### Compositions in the granules

The pellets recovered were subjected to infrared spectra analyses (Figure S4), X-ray diffraction (Figure S5) and elemental analyses. In terms of the works performed by Çelen et al. (2007) and Pastor et al. (2010), the possible minerals precipitated in struvite recovery from digested swine wastewater were struvite, as well as K-struvite ( $\text{MgKPO}_4 \cdot 6\text{H}_2\text{O}$ , MKP), and amorphous calcium phosphate (ACP,  $\text{Ca}_3(\text{PO}_4)_2 \cdot x\text{H}_2\text{O}$ ), which were also verified by our previous works (Ye et al, 2011; Shen et al., 2015). 91.61-96.74% struvite, 0.74-1.74% MKP and 0.26-3.74% ACP were detected, as displayed in Table 3. As to organic matters, 0.31-1.08% was observed (Table S2).

The elemental distribution along the radius direction in the coating-growth granule was examined, and the subsequent image illustrated that Ca and C had higher contents in the interior than in the exterior (Figure 5 and Table S2). Considering that inner clusters in the coating-growth granule contained much more nano-scale ACP (Lin et al., 2014) and suspended organic matters than the outer layer (Table S2), it was conclusive from another aspect that the coating-growth granules might be formed with aggregates or cluster-agglomerating granules as the nuclei.

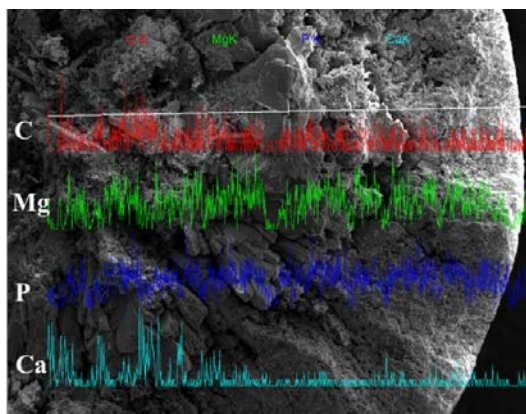


**Figure 5.** Elemental distribution along the radius direction in the coating-growth granule.

## DISCUSSION

Fluidized granulation process in the gas-solid fluidized bed has been extensively investigated and applied at a massive scale in the manufacture of detergents, agricultural chemicals, foods and pharmaceutical products (Wang et al., 2013; Coronel-Aguilera and Martín-González, 2015). Granule formation and subsequent growth progresses in the gas-solid fluidized bed primarily go through three stages: nucleation, transition, and granule growth (Hemati et al., 2003). With regard to the liquid-solid fluidized bed, the understanding of solid granulation is still limited. This is because liquid-solid fluidization system is generally considered as “particulate fluidization” and is hard for granulation, in which solid particles are uniformly distributed in space and time (An et al., 2007). Therefore, the mechanisms in the gas-solid fluidized bed, including particle surface wetting, granule nuclei formation and granule growth (Chen et al., 2009a; da Silva et al., 2014), are not effective to predict struvite granulation in the liquid-solid fluidized bed.

The present study used the image processing to investigate the morphology changes of struvite particles in the fluidized bed. From Figure 1 and 2, it was clearly that struvite granule formation was a process consisting of four stages: aggregation, aggregate compaction, cluster agglomeration and coating growth. These stages can occur subsequently or in parallel, which are different from the granulation in gas-solid fluidized bed where agglomeration and coating occurred subsequently (Saleh et al., 2003; Chen et al., 2009b). Under the conditions of 30-80 mm/s up-flow rates, the flow sustained 600-876 g/L granular solids, with the diameters of two types of pellets (cluster-agglomerating and coating-growth granules) at 1.186-1.872 mm (Table 1). Elemental distribution along the radius direction in the coating-growth granule (Figure 5), combining with granule structure (Figure S3), crushing strength (Figure 4) and evolution process (Figure 2) confirmed that coating-growth granules were formed with cluster-agglomerating granules as the nuclei.

Based on the above statement, a relatively integral process of struvite crystal granulation in the fluidized bed was elucidated as shown in Figure 6. Under appropriate conditions (supersaturation, pH etc.), struvite nuclei are continuously generated in the bottom of the fluidized bed and disperse to the whole reactor driven by the upward flow. The fine crystal embryos spontaneously go through crystal growth stage to form detectable crystals (Le Corre et al., 2009). Due to the typical orthorhombic structure, struvite nuclei are prone to crystallized into needle or rod shapes, and aggregate at the corners or edges of crystals (Ye et al., 2014). With the growth of aggregates and the functions of hydraulic turbulence, aggregate compaction gradually starts to dominate in the top section. In case compact aggregates are heavier than the uplift forces that the flow provides, compact aggregates will descend to the middle section and continue the transition to the next stage.

In the cluster-agglomeration stage, lots of compact aggregates collide, fragment, and are compressed to form clusters, in which the interaction between agglomeration and breakup forces plays a crucial role on granule formation. In case of primary struvite nuclei as the binder, cluster-agglomerating granules will be formed by coalescence of compact clusters, through the mechanism of solid-liquid bridging (Hemati et al., 2003; Balakin et al., 2015). The heavier cluster-agglomerating granules will thereafter sink to the bottom section to continue the remaining process. In the last stage, the mode of coating-growth occurs by layering of primary nuclei or by subsequent crystal coalescence (Pauli-Bruns et al. 2010; Yamada et al., 2014), which suggests that the coating-growth granule is formed with the cluster-agglomerating granule as the nuclei. Once the granules are big enough to exceed the uplift limit that the flow can afford, the granules will settle down and be harvested at intervals. Simultaneous and subsequent occurrence of these stages was observed in the present study (Table 1).

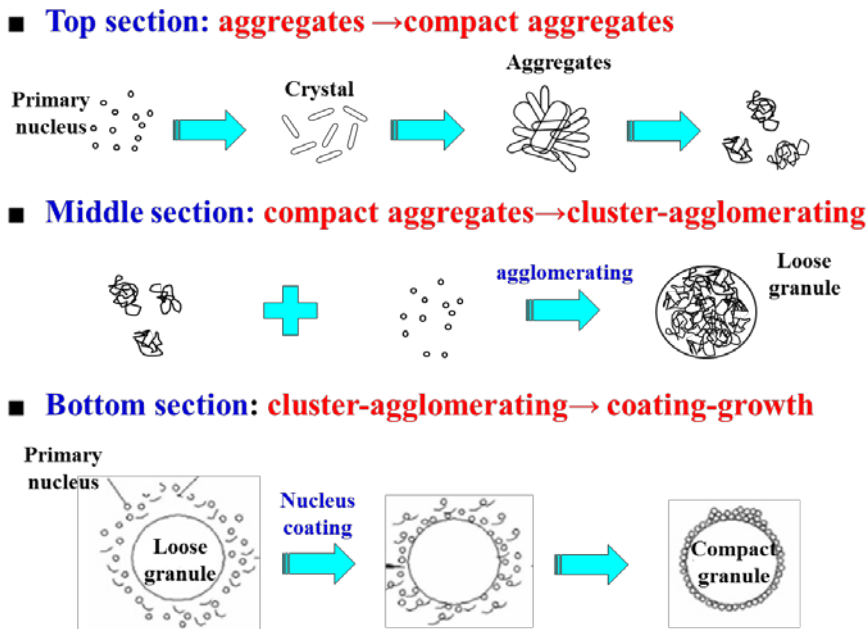


**Figure 6.** Schematic illustration for struvite granulation in the fluidized bed.

The information of granule grow rates is very practical and useful, since it provides better description of the granule growth in the fluidized bed, and the parameters for various operational modes can be adjusted optimally so as to harvest desired products. For the granulation in gas-solid fluidized bed, the growth rates of the pellets include the population growth, mass increase and particle size enlargement (Avilés- Avilés et al., 2015). Similarly, the mean growth rates of struvite granule were calculated, as shown in Table 1. Theoretically, granule growth governed by agglomeration results in coalescing compact clusters, leading to larger size enlargement, more population reduction and less mass increase (Hemati et al., 2003; da Silva et al., 2014). Coating corresponds to the deposition of ingredients on the entire surface of pellets, normally resulting with less size increase, smaller number reduction and larger mass increase (Hemati et al., 2003; da Silva et al., 2014). However, the growth rates ( $v_m$ ,  $v_n$  and  $v_r$ , in Table 1) obtained in the present study displayed different profiles, compared to the gas-solid granulation modes. This is because in conventional modes, agglomeration and coating growth occur independently or subsequently. Nevertheless, struvite particles evolve with the processes of agglomeration and coating simultaneously (Table 1). Besides, different from the conventional granulation mechanisms with definite quantities of nuclei for population balance (Galbraith and Schneider, 2014; Triger et al., 2012), struvite nuclei are continuously generated in the fluidized bed so that the nuclei population is

unbalanced and hard to be measured. Hence, in order to get the variation rules of growth rates in struvite granulation process, strictly controlled experiments will be conducted in the near future.

## CONCLUSION

Image processing, coupling with composition analysis, was adopted to describe the characteristics of granules in the process of struvite recovery from swine wastewater using fluidized bed reactor. Up-flow rates of 30-80 mm/s in the fluidized bed sustained 600-876 g/L granular solids, and harvested pellets with the size range of 1.186-1.872 mm. Struvite particles in the fluidized bed evolved into four subsequent states, including aggregation, aggregate compaction, cluster-agglomerating and coating growth. Different from the conventional granulation mechanisms, struvite particles evolved with the processes of agglomeration and coating, simultaneously. Results revealed that the coating-growth granules were formed with compact aggregates or cluster-agglomerating granules as the nuclei. A process model for struvite granulation in the fluidized bed was developed to better understand the mechanisms of struvite granulation.

## ACKNOWLEDGEMENT

This work was supported by the Xiamen Science and Technology Planning Project (No. 3502Z20162002) and the Fujian Science and Technology Plan Project (No. 2014Y0076).

## REFERENCES

- An, X., Liu, M., Fu, Y. 2007 Clustering behavior of solid particles in two-dimensional liquid-solid fluidized-beds. *China Particuology* **5**(5), 305-311.
- American Public Health Association (APHA). 1998 Standard Methods for the Examination of Water and Wastewater, 20th ed. *American Public Health Association/ Water Pollution Control Federation*.
- Avilés- Avilés, C., Dumoulin, E., Turchiuli, C. 2015 Fluidized bed agglomeration of particles with different glass transition temperatures. *Powder Technology* **270**(Part B), 445-452.
- Balakin, B.V., Shamsutdinova, G., Kosinski, P. 2015 Agglomeration of solid particles by liquid bridge flocculants: Pragmatic modelling. *Chemical Engineering Science* **122**(27), 173-181.
- Chen, Y., Yang, Y., Dave, R.N., Pfeffer, R. 2009a Granulation of cohesive geldart group C powders in a Mini-Glatt fluidized bed by pre-coating with nanoparticles. *Powder Technology* **191**(1-2), 206-217.
- Chen, Y., Yang, J., Mujumdar, A., Dave, R. 2009b Fluidized bed film coating of cohesive Geldart group C powders. *Powder Technology* **189**(3), 466-480.
- Coronel-Aguilera, C.P., Martín-González, M.F.S. 2015 Encapsulation of spray dried  $\beta$ -carotene emulsion by fluidized bed coating technology. *Lebensmittel-Wissenschaft und-Technologie* **16**(1), 187-193.
- da Silva, C.A.M., Butzge, J.J., Nitz, M., Taranto, O.P. 2014 Monitoring and control of coating and granulation processes in fluidized beds – A review. *Advanced Powder Technology* **25**(1), 195-210.
- Fattah, K.P., Mavinic, D.S., Koch, F.A. 2012 Influence of process parameters on the characteristics of struvite pellets. *Journal of Environmental. Engineering-ASCE* **138**(12), 1200-1209.
- Forrest, A.L., Fattah, K.P., Mavinic, D.S., Koch, F.A., 2008. Optimizing struvite production for phosphate recovery in WWTP. *Journal of Environmental. Engineering-ASCE* **134**(5), 395-402.
- Galbraith, S.C., Schneider, P.A., Flodd, A.E. 2014 Model-driven experimental evaluation of struvite nucleation, growth and aggregation kinetics. *Water Research* **56**(6), 122-132.
- Gilbert, N. 2009 Environment: the disappearing nutrient. *Nature* **461**(7265), 716-718.

- Huang, H., Mavinic, D.S., Lo, K.V., Koch, F.A. 2006 Production and basic morphology of struvite crystals from a pilot-scale crystallization process. *Environmental Technology* **27**(3), 233-245.
- Hemati, M., Cherif, R., Saleh, K., Pont, V. 2003 Fluidized bed coating and granulation: influence of process-related variables and physicochemical properties on the growth kinetics. *Powder Technology* **130**(1-3), 18-34.
- Iqbal, M., Bhuiyan, H., Mavinic, D.S. 2008 Assessing struvite precipitation in a pilot-scale fluidized bed crystallizer. *Environmental Technology* **29**(11), 1157-1167.
- Le Corre, K.S., Valsami-Jones, E., Hobbs, P., Parsons, S.A. 2009 Phosphorus recovery from wastewater by struvite crystallization: A review. *Critical Review of Environmental Science and Technology* **39**(6), 433-477.
- Lin, K., Wu, C., Chang, J. 2014 Advances in synthesis of calcium phosphate crystals with controlled size and shape. *Acta Biomaterialia*. **10**(10), 4071-4102.
- Pauli-Bruns, A., Knop, K., Lippold, B.C. 2010 Preparation of sustained release matrix pellets by melt agglomeration in the fluidized bed: influence of formulation variables and modelling of agglomerate growth. *European Journal of Pharmaceutics & Biopharmaceutics* **74**(3), 503-512.
- Rahaman, M.S., Mavinic, D.S., Meikleham, A., Ellis, N. 2014 Modeling phosphorus removal and recovery from anaerobic digester supernatant through struvite crystallization in a fluidized bed reactor. *Water Research* **51**(51), 1-10.
- Saleh, K., Steinmetz, D., Hemati, M. 2003 Experimental study and modeling of fluidized bed coating and agglomeration. *Powder Technology* **130**(1-3), 116-123.
- Shen, Y., Ye, Z.L., Ye, X., Wu, J., Chen, S.H. 2015 Phosphorus recovery from swine wastewater by struvite precipitation: compositions and heavy metals in the precipitates. *Desalination Water Treatment*, DOI: 10.1080/19443994.2015.1035342.
- Triger, A., Pic, J., Cabassud, C. 2012 Determination of struvite crystallization mechanism in urine using turbidity measurement. *Water Research* **46**(18), 6084-6094.
- Wang, G., Yang, L., Lan, R., Wang, T., Jin, Y. 2013 Granulation by spray coating aqueous solution of ammonium sulfate to produce large spherical granules in a fluidized bed. *Particuology* **11**(5), 483-489.
- Walker, G.M., Magee, T.R.A., Holl, C.R., Ahmad, M.N., Fox, N., Moffatt, N.A. 1997 Compression testing of granular NPK fertilizers. *Nutrient Cycling in Agroecosystems* **48**(3), 231-234.
- Yamada, N., Mise, R., Ishida, M., Iwao, Y., Noguchi, S., Itai, S. 2014 Effects of the centrifugal coating and centrifugal fluidized bed coating methods on the physicochemical properties of sustained-release microparticles using a multi-functional rotor processor. *Advanced Powder Technology* **25**(1), 430-435.
- Ye, Z.L., Chen, S., Lu, M., Shi, J.W., Lin, L.F., Wang, S.M. 2011 Recovering phosphorus as struvite from the digested swine wastewater with bittern as a magnesium source. *Water Science & Technology* **64**(2), 334-340.
- Ye, Z., Shen, Y., Ye, X., Zhang, Z., Chen, S., Shi, J. 2014 Phosphorus recovery from wastewater by struvite crystallization: Property of aggregates. *Journal of Environmental Sciences* **26**(4), 991-1000.